

PS Late Pleistocene Bryant Canyon Turbidite Facies: Implications for Gulf of Mexico Mini-Basin Petroleum Systems*

John E. Damuth¹, Hilary C. Olson¹, and C. H. Nelson²

Search and Discovery Article #11202 (2019)**

Posted March 4, 2019

*Adapted from poster presentation given at 2018 AAPG Annual Convention & Exhibition, Salt Lake City, Utah, May 20-23, 2018

**Datapages © 2019 Serial rights given by author. For all other rights contact author directly. DOI:10.1306/11202Damuth2019

¹Institute for Geophysics, University of Texas at Austin, Austin, Texas, United States (damuth@uta.edu)

²Instituto Andaluz de Ciencias de la Tierra, University of Granada, Granada, Spain

Abstract

The Western Ancestral Mississippi shelf-margin delta fed the Bryant Canyon/Fan Turbidite System in the intraslope basin province of the northwestern Gulf of Mexico (GOM) during the Penultimate Glacial (MIS 6) lowstand of sea level. The Bryant Submarine Canyon links a chain of 15 fill-and-spill mini-basins on the continental slope. On the upper and lower continental slope, these mini-basins are narrow (1-3 km), elongate (3-6 km), and follow salt ridges. On the middle slope, the mini-basins are larger (8-15 km), semi-circular basins. Interpretation of seismic facies displayed by the mini-basin deposits reveal three main depositional facies: (1) ponded turbidites (T), (2) mass transport-deposits (MTD), and (3) bypass channelized turbidites (C). These deposits are capped at many locations by thick deposits of intrabasinal, muddy MTD wedges sourced from the high-relief walls of the mini-basins. These intrabasinal MTD wedges are interbedded with the externally derived basin deposits. Extrabasinal MTD deposits were derived from shelf-margin delta or canyon-wall failures and then transported through bypass channels to the mini-basin depocenters.

The T and MTD facies deposits each make up about 40% of the basin fill and the C facies deposits comprise about 20%. The T facies deposits form perched lobes at canyon inlets into basins and ponded units on the distal sides of the basins. Channels in the C facies are similar in width (500-2000 m) and relief (20-100 ms) to channels in productive GOM subsurface mini-basins. Syntectonic activity of salt diapirs typically began midway through filling of the Bryant Canyon mini-basins and then preferentially uplifted the northern portions of basin deposits. Salt-tectonic activity in the Bryant Canyon area has caused greater basin relief and thicker capping MTDs than in subsurface mini-basins to the east (e.g., Brazos Trinity Basin IV) or west (e.g., Mississippi Canyon). The modern Bryant Canyon mini-basins exhibit the same scales (e.g., basin size, facies thickness, and channels) and depositional facies as older GOM subsurface mini-basins. Thus, the Bryant Canyon mini-basins provide excellent “modern” analogues for the subsurface Miocene to Pleistocene GOM chains of mini-basins such as in the Mississippi Canyon area. The youngest Bryant T facies deposits and their overlying incised, thick, channel deposits contain the most sand-prone facies and suggest the best potential for petroleum reservoirs in subsurface mini-basins.

1

ABSTRACT

Late Pleistocene Bryant Canyon Turbidite Facies: Implications for Gulf of Mexico Mini-basin Petroleum Systems

John E. Damuth^{1,2}, Hilary Clement Olson^{1,3,4} and C. Hans Nelson⁵

¹ Institute for Geophysics, Jackson School of Geosciences, The University of Texas at Austin, 10100 Burnet Rd., Austin, TX 78758

² Department of Earth and Environmental Sciences, University of Texas at Arlington, P.O. Box 19049, Arlington, TX 76019

³ Center for Petroleum and Geosystems Engineering, Cockrell School of Engineering, The University of Texas at Austin, 200 Dean Keeton St., Austin, TX 78712

⁴ Bureau of Economic Geology, Jackson School of Geosciences, The University of Texas at Austin, Box X, Austin, TX 78713

⁵ Instituto Andaluz de Ciencias de la Tierra, Av. de las Palmeras, 4, 18100 Armilla, (Granada) Spain.

The Western Ancestral Mississippi shelf-margin delta fed the Bryant Canyon/Fan Turbidite System in the intraslope basin province of the northwestern Gulf of Mexico (GOM) during the Penultimate Glacial (MIS 6) lowstand of sea level. The Bryant Submarine Canyon links a chain of 15 fill-and-spill mini-basins on the continental slope. On the upper and lower continental slope, these mini-basins are narrow (1-3 km), elongate (3-6 km), and follow salt ridges. On the middle slope, the mini-basins are larger (8-15 km), semi-circular basins. Interpretation of seismic facies displayed by the mini-basin deposits reveal three main depositional facies: (1) ponded turbidites (T), (2) mass-transport deposits (MTD), and (3) bypass channelized turbidites (C). These deposits are capped at many locations by thick deposits of intrabasinal, muddy MTD wedges sourced from the high-relief walls of the mini-basins. These intrabasinal MTD wedges are interbedded with the externally derived basin deposits. Extrabasinal MTD deposits were derived from shelf-margin delta or canyon-wall failures and then transported through bypass channels to the mini-basin depocenters. The T and MTD facies deposits each make up about 40% of the basin fill and the C facies deposits comprise about 20%. The T facies deposits form perched lobes at canyon inlets into basins and ponded units on the distal sides of the basins. Channels in the C facies are similar in width (500-2000 m) and relief (20-100 ms) to channels in productive GOM subsurface mini-basins. Syntectonic activity of salt diapirs typically began midway through filling of the Bryant Canyon mini-basins and then preferentially uplifted the northern portions of basin deposits. Salt-tectonic activity in the Bryant Canyon area has caused greater basin relief and thicker capping MTDs than in subsurface mini-basins to the east (e.g., Brazos Trinity Basin IV) or west (e.g., Mississippi Canyon). The modern Bryant Canyon mini-basins exhibit the same scales (e.g., basin size, facies thickness, and channels) and depositional facies as older GOM subsurface mini-basins. Thus, the Bryant Canyon mini-basins provide excellent “modern” analogues for the subsurface Miocene to Pleistocene GOM chains of mini-basins such as in the Mississippi Canyon area. The youngest Bryant T facies deposits and their overlying incised, thick, channel deposits contain the most sand-prone facies and suggest the best potential for petroleum reservoirs in subsurface mini-basins. [For detailed discussion of this study please see: Nelson, C.H., Damuth, J.E., and Olson, H.C., 2018, Late Pleistocene Bryant Canyon turbidite system: Implications for Gulf of Mexico minibasin petroleum systems; Interpretation, V. 6, No. 2, \(May 2018\), p. 1-26.](#)



2

Objectives of the Study

1. Integrated analysis of the Bryant Canyon and East Canyon turbidite systems to provide a modern analogue for similar deeply buried prospective systems, e.g., the ultra-deep mid-to-late Miocene, Pliocene and early Pleistocene petroleum plays in the northern GOM.

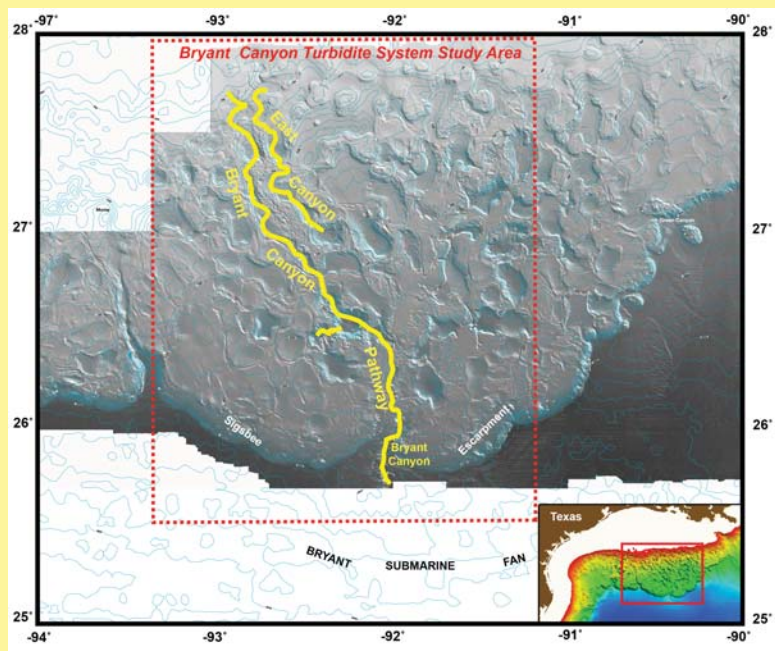
2. Characterize and compare the morphology and depositional facies of the wide variety of Bryant Canyon mini-basins, bypass channels, and connecting canyon thalwegs based on observed seismic facies.

3. Provide reservoir relevant parameters of the modern Bryant Canyon thalwegs and mini-basins, and compare these to those of the Miocene-to-Pleistocene subsurface turbidite systems, which appear to have had the same morphological components, scales of features and sedimentary facies. To achieve this, we compare the characteristics for the sand prone facies of the Bryant Canyon turbidite system with those of other classically described systems in the GOM. Our study provides detailed new data that can be utilized for reservoir prediction in giant petroleum plays found in the ultra-deep northern GOM, such as Thunder Horse, Mad Dog, and Thunder Horse North.

4. This synthesis advances the study of mini-basins because it traces an entire system from a shelf margin delta source through 15 mini-basins and connecting canyons into a final depositional sink of the sand-rich Bryant Fan.

3

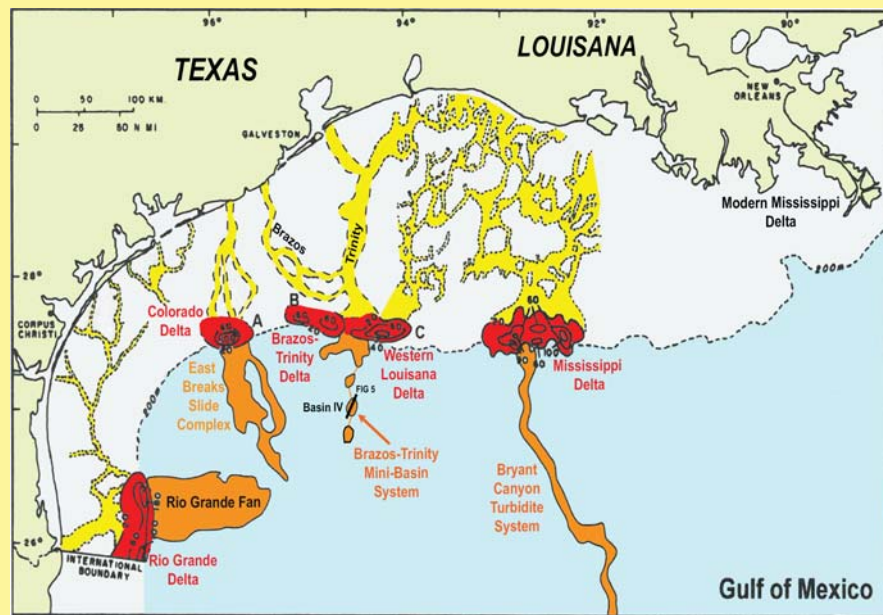
Location of Study Area



Location of the Bryant Canyon turbidite system in the northern Gulf of Mexico intraslope basin province (location in inset). Dashed red box shows location of study area and is shown in detailed map (No. 10) in center panel. Yellow lines show axes of Bryant Canyon and East Canyon. Bryant Canyon can be traced continually from the continental shelf break across the entire intraslope basin province for 200 km through 15 mini-basins to the Bryant Submarine Fan on the Sigsbee Abyssal Plain. In contrast, the East Canyon system extends only 90 km through 5 mini-basins and ends on the middle slope in the Calcasieu Basin (E5). Bathymetric contours (100 m interval) from Sandwell and Smith (1997). Swath bathymetry (Sea beam) from NOAA (NGDC). Inset map from Lui and Bryant (2006).

4

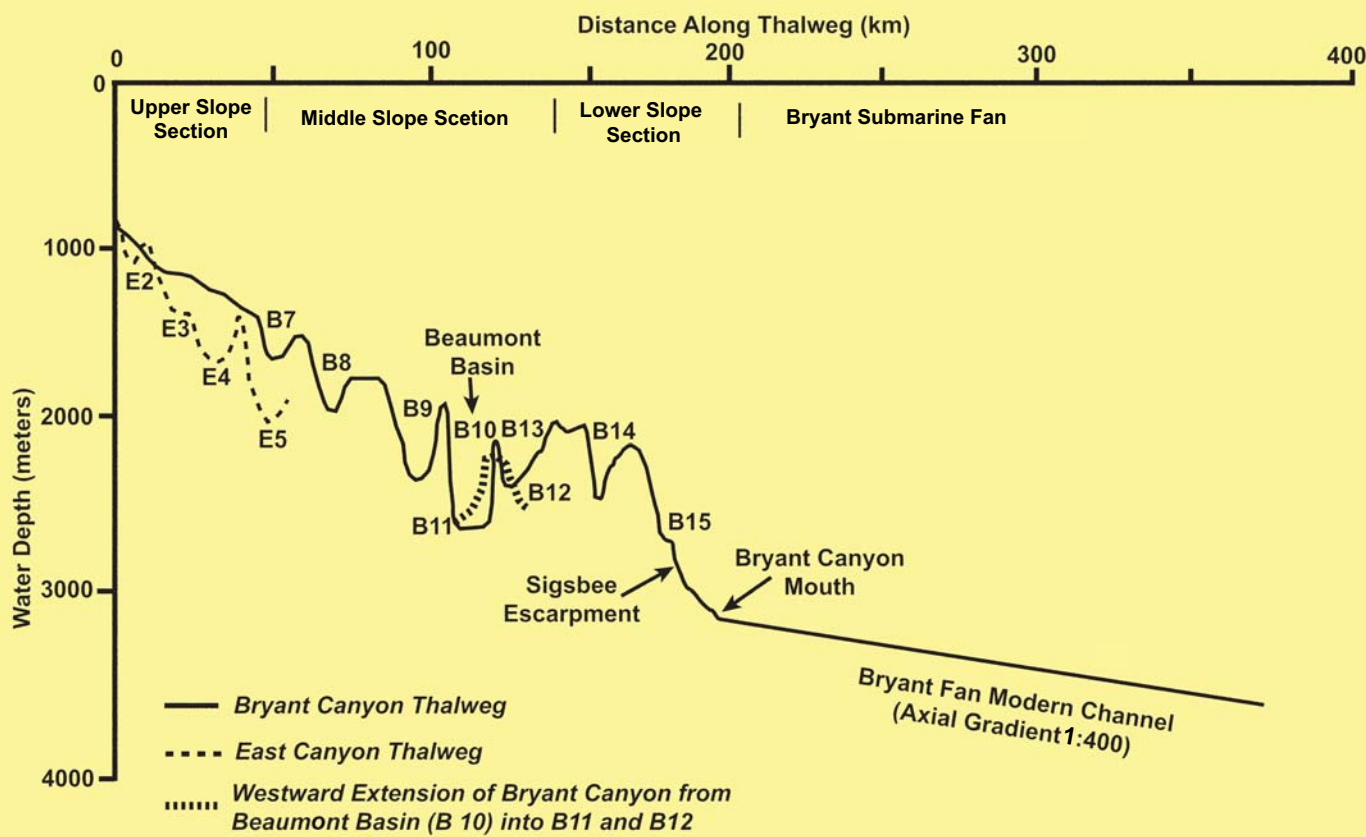
Fluvial Systems Feeding Bryant Canyon



Locations of the youngest incised/extended fluvial systems (yellow) and shelf-margin deltas (red) that formed on the continental shelf during lowered sea level of the Last Glacial (Wisconsin) (MIS 2) and the Penultimate Glacial (MIS 6). The ancestral Mississippi River fluvial system and delta fed the Bryant Canyon turbidite system during these glacial-eustatic lowstands. (Map modified from Suter, 2003). Large volumes of sandy sediments were transported by turbidity currents and related gravity-controlled mass flows (e.g., mass-transport deposits) from shelf-edge deltas downslope through Bryant Canyon and other mini-basin systems to deep-sea fans such as Bryant Fan. Thick sand units were ponded in the mini-basins (see seismic profiles in Nos. 8 & 10 of center panel).

5

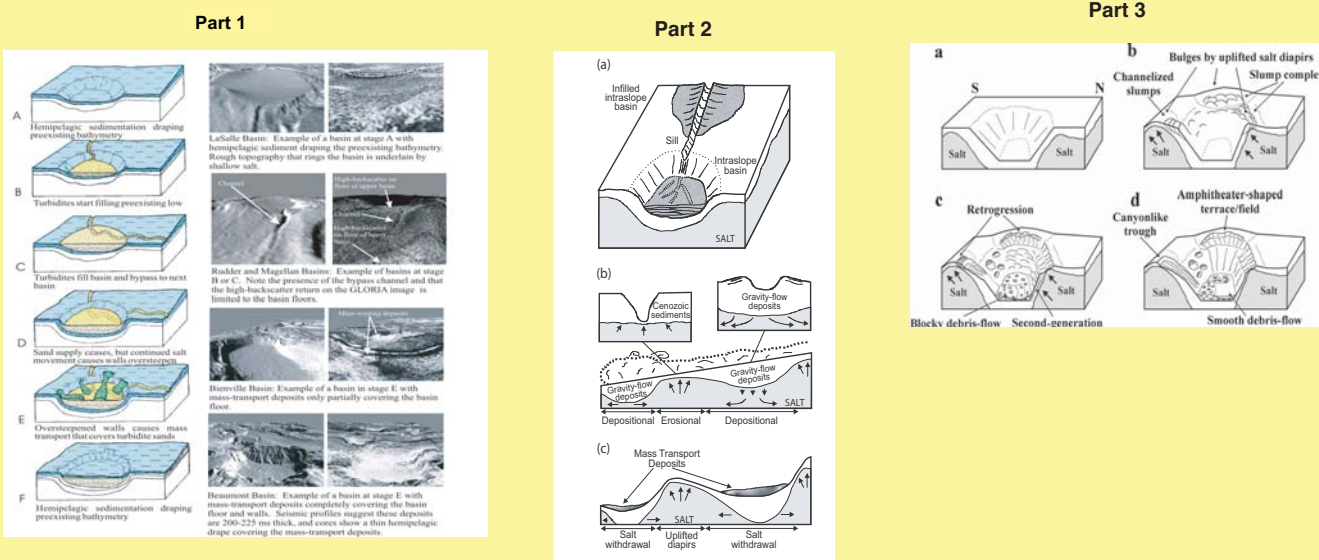
Bryant Canyon/Fan Thalweg



Continuous plots of the modern thalwegs of the Bryant (solid line) and East (dashed line) canyons derived from multibeam bathymetry (No. 10 in center panel). The East Canyon is limited to the upper continental slope, whereas the Bryant Canyon crosses the entire slope. Note that the normally continuous thalweg gradients of the Bryant and East canyon pathways have been disrupted by post depositional salt tectonics. The locations of the canyon and mini-basin thalwegs are shown on the bathymetric map in the center panel. The axial thalweg of the modern channel on the Bryant Submarine Fan is also shown extending downslope from the Bryant Canyon mouth in the Sigsbee Escarpment. Modified from Twichell, Nelson & Damuth (2000).

6

Background: Formation of Bryant Canyon Mini-Basins



Models showing the interplay between halokinetic salt tectonics, turbidity-current fill-and-spill process, and mass-transport deposition (MTD) in the intraslope salt withdrawal mini-basins of the Bryant Canyon turbidite system.

Part 1. Conceptual model of the evolution of mini-basins along the Bryant Canyon Pathway. Different modern basins from this continental slope are shown as examples of 4 of the 6 different conceptual stages (A, B, C, E) (after Twichell, Nelson & Damuth, 2000).

Part 2. Interplay of fill-and-spill mini-basin deposition and erosion with salt tectonics. (a) Shows a plan view of an infilled mini-basin with a bypass channel feeding a ponded mini-basin downstream. (b) Shows the cross section of canyon erosion of salt sills between mini-basins and the bypass channel deposition within mini-basins during glacial sea-level lowstand. (c) Shows a cross section of the mass-transport processes caused by basin-wall instability that results from sediment loading of basin infill, salt withdrawal beneath mini-basins and uplifted salt diapirs between mini-basins during interglacial sea-level highstand (after Tripsanas et al., 2004b).

Part 3. Evolution of Bryant Canyon mini-basins during oxygen-isotope Stage 2 sea-level lowstand. (a) Basin morphology at the beginning of lowstand. (b) Seaward mobilization of salt masses increases basin wall gradients causing deep, rotational slump complexes. (c) Deposition of MTD's at the foot of walls results in successive sets of retrogressive translational slumps. (d) Present basin morphology and increased stability because of reduced salt mobility during the Holocene (after Tripsanas et al., 2004a).

Latest Pleistocene Bryant Canyon Turbidite Facies: Implications for Gulf of Mexico Petroleum Systems

John E. Damuth,^{1,3} Hilary Clement Olson^{1,2} and C. Hans Nelson⁴

¹Institute for Geophysics, Jackson School of Geosciences and ²Center for Petroleum and Geosystems Engineering, The University of Texas at Austin;

³Department of Earth and Environmental Sciences, University of Texas at Arlington, ⁴Instituto Andaluz de Geosciences, Granada, Spain

7

Interpretation of Depositional Facies

Prather et al. (1998) classified the seismic-facies in Gulf of Mexico mini-basins and interpreted the depositional facies of the basins based on the seismic facies. We have utilized their classification and their interpretation of GOM mini-basin depositional facies to interpret the depositional facies of the Bryant Canyon system. Beaumont Basin (Nos. 8 & 10, to the right) is the best location to define the seismic and depositional facies for the mini-basins and connecting canyons because it is the largest mini-basin (~15 km diameter) with most numerous lines and clearest seismic facies. Our classification (Table below) is slightly modified from that of Prather et al. (1998). We interpret four main depositional facies from the seismic facies observed in Beaumont Basin: (1) channelized turbidites with bypass channels (C), (2) ponded turbidites (T), (3) mass-transport deposits (MTD) and (4) undifferentiated interbeds (U) (see table and GYRE lines T7 and T2 below, also other lines to the right around Beaumont bathymetric map). Multiple units of various depositional facies are interbedded within the basin and are labelled MTD-1, MTD-2, etc., or T-1, T-2, etc., where 1 is the relatively youngest, with 2, 3, 4, etc. being subsequently older units. We have designated each discrete depositional facies as a facies unit (e.g., T-1 facies unit). In the Beaumont Basin fill, the youngest depositional facies unit is MTD-1, which sometimes is combined with or overlain by the U facies unit. The C facies unit is the second youngest unit and underlies MTD-1/U. Interbedded facies units MTD-2 to MTD-5 and T-1 to T-5 are found beneath the younger units.

Channelized Turbidite Facies Units (C) (green shading)

The distinguishing geometric characteristics for the seismic facies of Unit C are the high-amplitude U- and V-shaped reflections, which are interpreted as channels (blue markings). The C facies unit also contains interbedded zones with a wide variety of reflections similar to those observed in the MTD, U and T facies units. However, the character of C facies unit is generally more horizontal and parallel bedded than the MTD facies unit, but is less continuous, less parallel with lower amplitude reflections than the T facies unit.

Ponded Turbidite Facies Units (T) (yellow shading)

In general, the T facies unit is characterized by seismic facies which display a geometry of horizontal, parallel, high-amplitude and continuous reflections. In areas of salt tectonic activity, the reflections are inclined and have undulations and contortions. These become progressively greater with depth because of increased salt tectonic disruption.

Mass-Transport Deposit Facies Units (MTD) (orange shading)

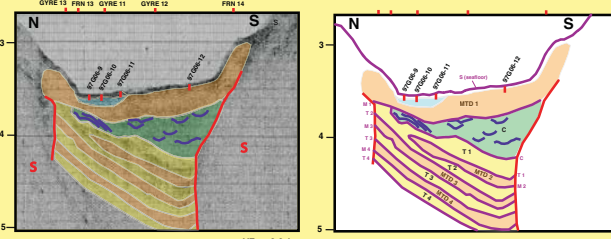
The seismic facies of the MTD facies units show hummocky, chaotic, contorted, semi-transparent, and discontinuous reflections and diffractions that are typical of mass-transport deposits. The down-lapping hummocky and chaotic wedges are most common at the bases of the steep mini-basin walls.

Undifferentiated Interbeds Facies Unit (U) (blue shading)

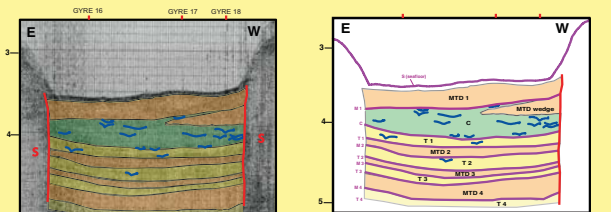
The uppermost deposits on the basin floor at many locations form the U facies unit. Seismic facies of the U facies unit are continuous, moderate-to-high-amplitude parallel reflections that are generally conformable with the seafloor. Cores from U facies contain a wide variety of sedimentary deposits, including hemipelagic sediment, silty turbidites, and uniform mud turbidites (unifites/homogenites).



Seismic Line GYRE 17



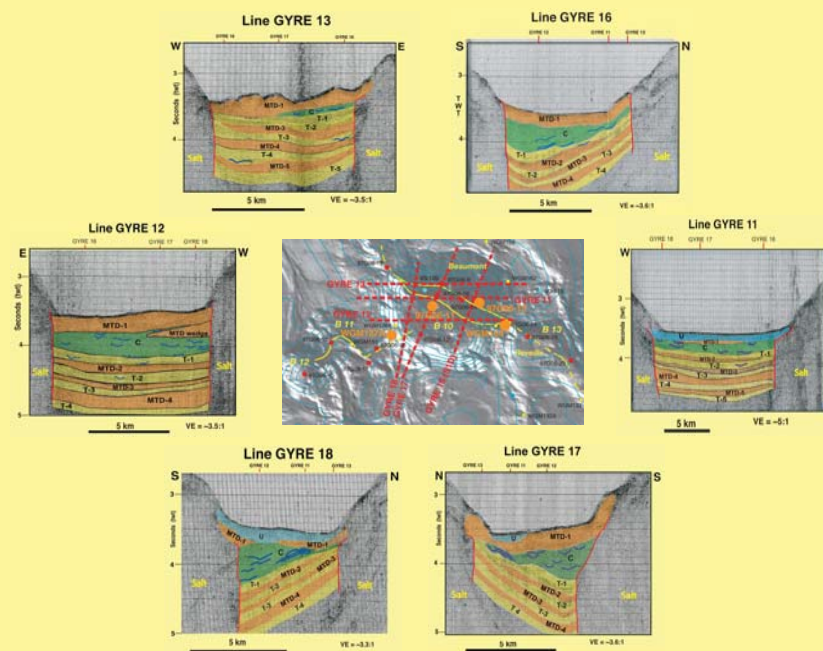
Seismic Line GYRE 12



Examples of interpreted seismic lines and corresponding line drawings showing types of depositional facies (e.g., C, MTD, T) interpreted on the seismic profiles interpreted for this study. The above lines are from the Beaumont Basin (B10) of the Bryant Canyon system. Locations of the lines are shown on the bathymetric maps shown in the center panel.

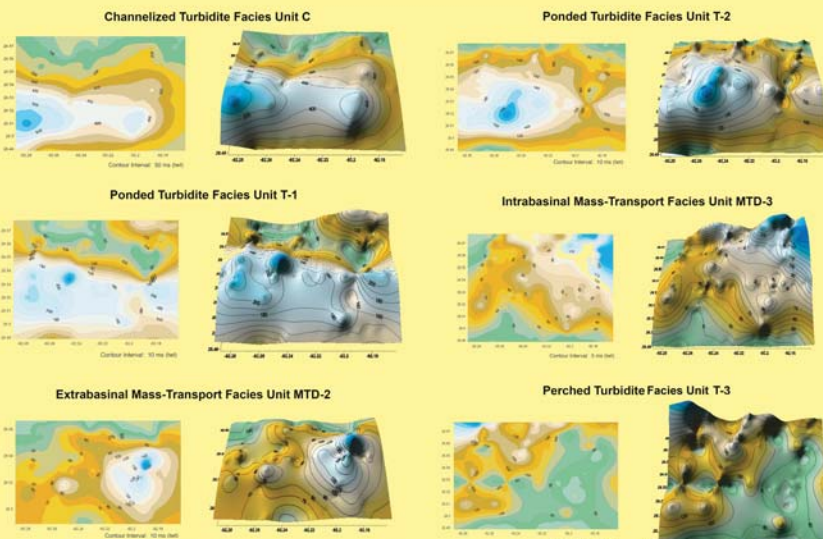
8a

Beaumont Basin Seismic Profiles



8b

Isopach Maps of Depositional Facies in Beaumont Basin (B10)



A series of isopach maps showing the thicknesses of these depositional facies units (C, MTD, T) in Beaumont Basin. Maps were compiled from seismic profiles shown in the upper figure plus some additional lines shown on large map at right (contours are in milliseconds of TWT; the interval (ms) is listed on each map; 3D perspective renditions of contour maps are illuminated from south to north).

8c

Depositional Facies and Processes in Beaumont Basin

The top figure shows 6 seismic profiles across Beaumont Basin which show interpretation of the depositional facies present based on the classification in No. 7 to the left (C, T-1, MTD-1, etc.). Locations of lines are shown on the swath-bathymetry map in the center (also see large bathymetric map to the right for location of the basin). Locations of piston cores are also shown and the large orange solid circles are shown on the panel to the right (No. 11, right panel). The bottom figure shows a series of isopach maps showing the thicknesses of these depositional facies units. Maps were compiled from seismic profiles shown in upper figure, plus some additional lines not shown (contours are in milli-seconds of TWT; the interval (ms) is listed on each map; 3D perspective renditions of contour maps are illuminated from south to north).

The thickness trend for the MTD-2 facies unit (No. 8, top figure) in Beaumont Basin indicates that it entered from the Bryant Canyon inlet to the basin and then ponded in depressions of the underlying T-2 facies unit. This thickness pattern of the MTD-2 facies unit indicates that it is an extrabasinal MTD derived upslope, then transported down the canyon to Beaumont Basin. In contrast, the large MTD-1 and MTD-3 facies units and small local wedges of MTD 1 are intrabasinal deposits that resulted from sediment failures derived from the Beaumont Basin wall. Basin-floor cores show that MTD 1 has been deposited up until the Holocene (Olson et al. 2016). The ponded nature represented by the T facies units is shown by the tabular and bulls-eye thickness patterns of isopachs (bottom figure) in the central basin. There is a thickening linear trend (~220 ms) in facies unit T4 along the north margin of the basin, which may be a channel complex that fed the thickest (300 m) part of T4 in the southeastern corner. Facies unit T-3 is thickest (220 ms) near the northwest entry point of the upstream Bryant Canyon. This trend suggests that turbidity-currents entering the basin from the northwest deposited a fan body in the northwest, and that sediments were drained from the southeast exit of the basin and did not pond. On the north side of the basin, significant portions of the upper part of the T-1 facies unit have been scoured out by apparent channel erosion (No. 8, top figure).

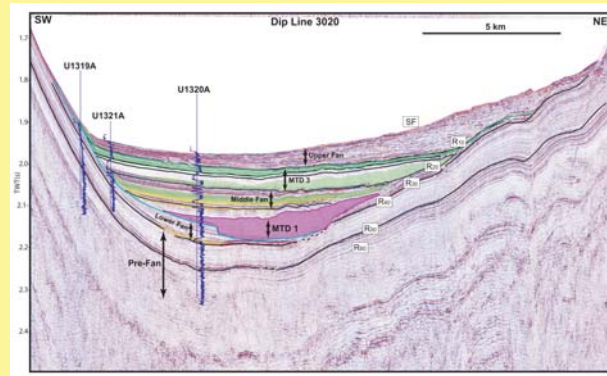
The salt tectonic uplift on the north has resulted in significant erosion by T-1 turbidites, which removed the MTD-2 facies unit and cut deeply into the T-2 facies unit. The combination of the tectonic uplift, loss of accommodation space and scour by mass-transport processes has resulted in the erosion of most of the T-1 facies unit in the northwest part of the basin. Increasing development of channels in the upper turbidite facies units and significant channel scour into the top of the T-1 facies unit indicate that Beaumont Basin was reaching the equilibrium point of its fill-and-spill history. Initiation of the C facies unit began with large channels that incised into the underlying T-1 facies unit. As a result, an extensive bypass channel system developed by the end of deposition of the T-1 facies unit. The bypass channel pathway can be traced as a deep, wide channel scour into T-1 on the northern portions of seismic profile segments and in the T-1 isopachs between the Bryant Canyon inlet in the northwest basin wall and the outlet in the east central basin wall. As the bypass channel system waned, progressively greater amounts of MTD-1 wedges extended into, and eventually dominated the youngest part of the C facies unit.

Alternating extrabasinal deposition of MTD units and T units occurred mainly during lowstands when the turbidite system was active, but periodic extrabasinal massive shelf-margin or canyon-wall failures traveled down canyons and deposited the ponded extrabasinal MTD facies units between the turbidite units. In contrast, the thick MTD-3 facies unit wedge extending from the northeast basin wall of Beaumont Basin indicates that this large MTD, as well as smaller MTD wedges interbedded into the turbidites, apparently resulted from basin-wall failures during low sea level. The north-to-south seismic profiles show that significant salt tectonics uplift of ~800-900 ms has taken place at the northern edge of Beaumont Basin (GYRE 16, 17, and 18). Significant uplift apparently has occurred after the deposition of the T-2 facies unit. This uplift is progressively greater to the north because the northernmost part of the MTD-2 facies unit is missing and the T-1 and T-2 facies units become amalgamated. Apparent erosional thinning of facies unit T-1 also occurs at the northern edge of the basin. Maximum truncation is observed in the C facies unit, where apparent syndetic erosion has reduced the thickness to <100 ms along the northern edge of the basin compared to 400 to 600 ms thickness at the southern edge of the basin. The erosional truncation observed in the MTD-2, T-1, and C facies units shows that significant tectonic uplift took place during this time of deposition. However, the uplift apparently slowed significantly and perhaps ceased during deposition of facies unit C.

NOTE: A detailed discussion of deposition in Beaumont Basin is given in our paper that is published in the May 2018 volume of Interpretation: Nelson, C.H., Damuth, J.E., and Olson, H.C., 2018, Late Pleistocene Bryant Canyon turbidite system: Implications for Gulf of Mexico minibasin petroleum systems; Interpretation, V. 6, No. 2, (May 2018), p. 1-26.

9

Brazos-Trinity Basin IV



Seismic-reflection dip line across Basin IV of the Brazos-Trinity Mini-basin Turbidite System in the northern Gulf of Mexico (modified from Expedition 308 Scientists, 2005). Location shown in No. 4, left panel. Reflections labeled 10-50, gamma well logs, and locations of IODP drill holes U1319A, U1320A and U1321A are from Expedition 308 Scientists (2005). Gamma logs are correlated with seismic facies of pre-fan, lower to upper fan and MTDs in the holes. Lower, Middle and Upper fan and MTD units 1 and 3 are based on interpretations of Badalini et al. (2000). Beaubouef and Friedman (2000) and Expedition 308 Scientists (2005). These fan and MTD facies units are equivalent to ponded turbidite (T) and mass-transport deposit (MTD) facies units of Bryant Canyon mini-basins. Although there are differences in the scale and length in the Brazos-Trinity and Bryant Canyon mini-basin systems, the basic types of T and MTD depositional facies are the same. Drill cores show that the Lower, Middle, and Upper fans in Basin IV are ponded turbidite facies (T) and these are interbedded with wedge-shaped MTD intrabasinal and tabular MTD extrabasinal facies like those in Bryant mini-basins. The IODP 308 drill holes in Basin IV deposits are similar to piston cores in the Bryant mini-basins (e.g., No. 11, right panel), and confirm that the intrabasinal MTDs are muddy debris flows from basin walls.

10

Proximal to Distal Depositional Facies in Mini-Basins

Map of the Bryant Canyon pathway study area (location in No. 2, left panel) showing bathymetry of the mini-basins along the canyons. The yellow lines trace the axes of Bryant and East canyons. Blue line to the south traces the axis of the modern fan channel-levee system of Bryant Submarine Fan, which extends downslope from the Bryant Canyon mouth and the Sigsbee Escarpment (see profile FRN 19). Interpreted seismic profiles are shown for selected seismic lines (red dashed lines and labels) down canyon. Basin labels B1 to B15 along Bryant Canyon and E1 to E5 along East Canyon identify mini-basins described in our study. Location of all seismic lines used in this study are shown by thin black lines. Bathymetric contours (blue) are from Sandwell and Smith (1997); contour interval = 100 m. Shaded swath bathymetry (Sea Beam) is from NOAA (NGDC).

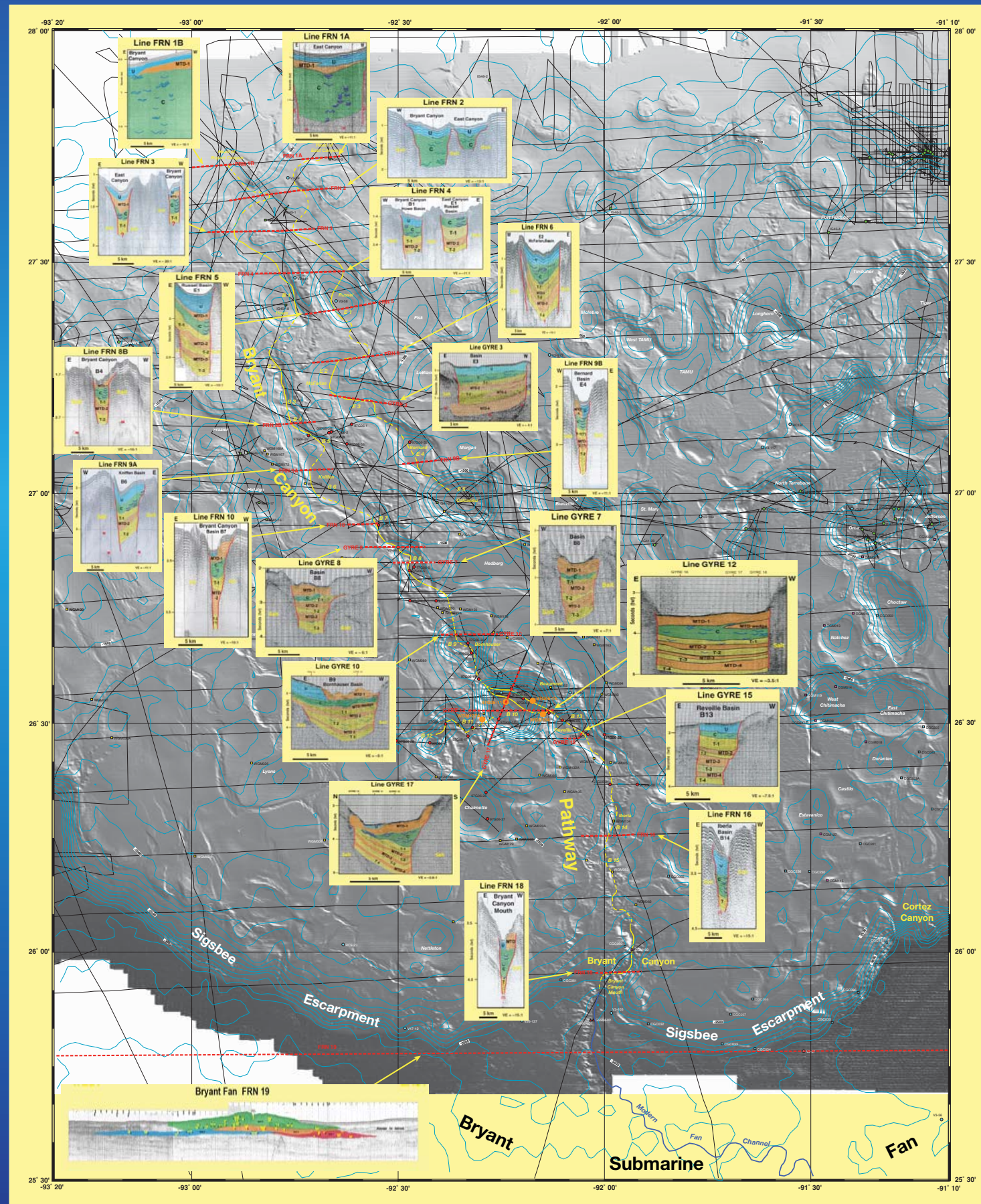
We cannot discuss these profiles in detail here and we give some general details below. Please see our detailed paper in the May issue of Interpretation for detailed discussion: Nelson, C.H., Damuth, J.E., and Olson, H.C., 2018, Late Pleistocene Bryant Canyon turbidite system: Implications for Gulf of Mexico minibasin petroleum systems; Interpretation, V. 6, No. 2, (May 2018), p. 1-26.

Similar to the Beaumont Basin (left), the MTD-1 and/or U facies units are the youngest facies units and extend from the basin floors up onto the basin walls in all the other mini-basins of Bryant and East canyons. The C facies unit is the second youngest unit and underlies MTD-1 and/or U facies units. Below these are variable numbers of interbedded MTD and T facies units, depending on the upper, middle or lower slope locations of the mini-basins. Numerical measurements and characteristics of the morphology, thicknesses of depositional facies units of each mini-basin and connecting canyon pathways are shown in Tables 1 and 2 (No. 11, right panel).

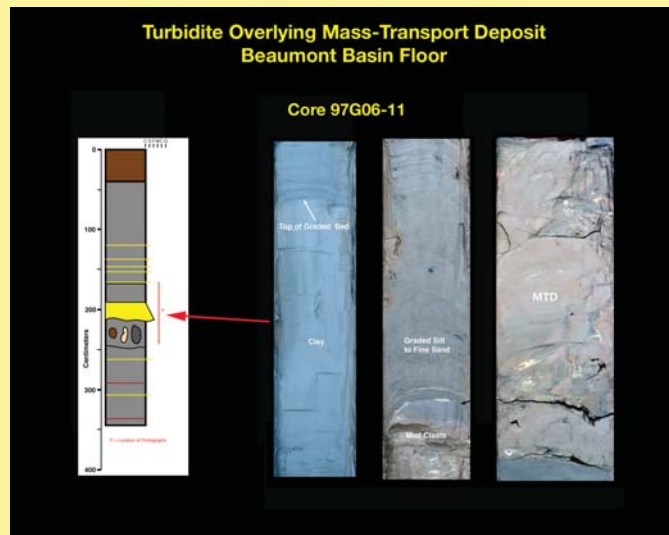
Both Bryant and East canyons originate as shallow valleys on the upper slope, but become narrower or deeper canyons as they progress downslope (see FRN 1A, 1B, 2, 3, and 4 on map). There is no salt tectonic activity on the uppermost slope and canyon relief is only ~100 m. Moving down the upper slope there is increasingly more relief (100-300 m), salt diapirism, and sediment infill. On the middle slope in Bryant Canyon, canyon wall relief reaches 400 m and the thickness of basin deposits is up to a maximum of 1750 ms (Table 1). On the lower slope along Bryant Canyon, both canyon and mini-basin wall relief vary from 300-600 m. See the plot of the canyon thalwegs in No. 5, left panel.

The depositional histories of Bryant and East canyon mini-basins are the result of an interplay between salt withdrawal tectonics and mini-basin fill-and-spill sedimentary processes. Syntectonic activity of salt withdrawal began once there was some deposition in the mini-basins. The greatest salt tectonic disruption and development of MTD facies occurred during the Penultimate Glacial (MIS 6) and early Last Interglacial (MIS 5) after the main deposition in the mini-basins took place. Sediment failures on canyon and mini-basin walls, and MTD deposition on basin floors have been the dominant sedimentary processes during the past ~130 kys since the major salt withdrawal.

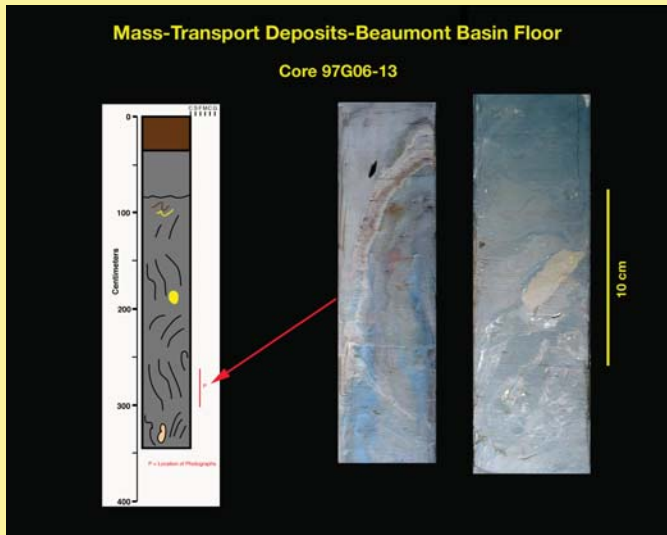
Table 3 (No. 11, right panel) compares channel characteristics of Bryant and East canyons with channels of other subsurface mini-basin systems (e.g., Auger etc.). Relief of channels is generally 50-100 ms and widths are typically ~1000 meters, but up to 2500 m maximum. All these channels have been fed by the large Ancestral Mississippi drainages. Because channel sizes are proportional to the size of turbidite systems, it is not surprising that the channel dimensions are similar throughout the north central GOM, where all the Miocene to Pleistocene mini-basins have been fed by the similar sized sediment source of the Ancestral Mississippi. In mini-basins where small rivers have fed the channel systems, for example, the Brazos-Trinity mini-basins (see No. 9, this panel), channel relief is lower (~50 m); or where the larger Mississippi River has fed Mississippi Fan during the Last Glacial (Wisconsin, MIS 2), channel relief is greater (up to 250 m) than Bryant Canyon or other Miocene to late Pleistocene mini-basins.



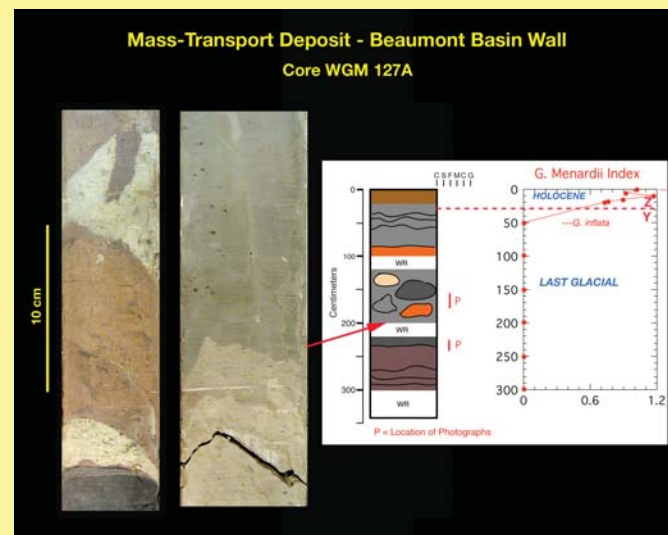
Late Quaternary Piston Cores from the Beaumont Basin



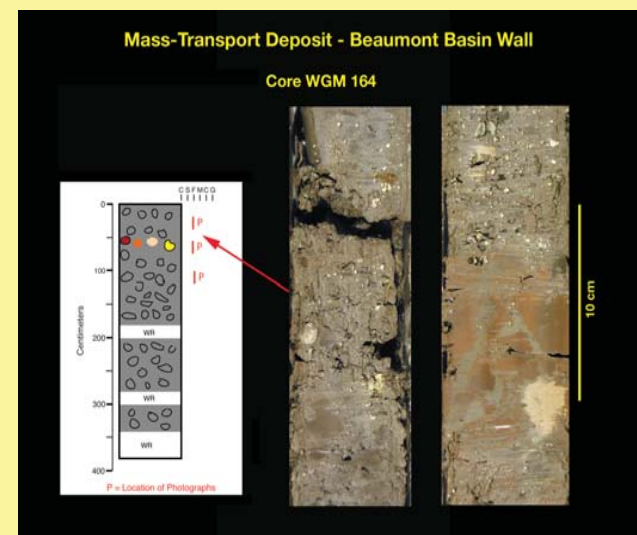
This core is from the middle of the intraslope basin floor in ponded sediments. The interval from 134-168 cm is a series of thin turbidites. 168-215 cm is a thick turbidite that overlies a muddy debris-flow deposit (215-274 cm). The interval below 244 cm also appears to be deposits of gravity-controlled flows.



Core from the edge of the basin in hummocky topography at the base of the basin wall. The mass-transport deposit of chaotic, deformed clays of the MTD appear to be a slump deposit. The 3.5 kHz seismic is consistent with a slump-debris flow deposit.



Core from western wall of basin. Whole core below 20 cm appears to be exotic mud clasts or blocks in a mass-transport deposit. The climatic curve on the right shows the MTDs occurred during the latest Last Glacial (Wisconsin; MIS 2).



Core from eastern wall of basin. Deformed mud clasts of variegated size, shape, color and composition in a muddy debris-flow deposit.

Core locations shown on Beaumont Canyon bathymetric map on center panel. Modified from Damuth & Olson (2015)

Characteristics of Bryant and East Canyons Mini-Basins and Channels

Mini-Basin	Seismic Profile Examples	Basin Floor Width (m)	Basin Floor Relief (m)	Maximum Basin Fill Thickness (m)	Types and Number of Depositional Facies Units per Basin				Thickness of Facies Units (m) in Each Basin				Channel Thaweg Dimensions	
					Ponded Turbidites (T)	Mass-Transport Deposits (MTD)	Mass-Transport Deposits (MTD)	Ponded Turbidites (T)	Ponded Turbidites (T) (Total)	Mass-Transport Deposits (MTD)	Mass-Transport Deposits (MTD) (Total)	Channelized Turbidites (C)	Width (m) (Max/Min)	Relief (m) (Max/Min)
B1	FRN 4	710	300/300	1215	2	2	1	300/175	525	200/150	350	400/350	1500/1000	40/25
B2		215	80/100	1650	3	3	1	400/140	760	200/200	700	100/100	2400/200	60/30
B3		2/4	300	1130	1	1	1	330/330	330	420/420	420	370/370	1200/1000	50/30
B4	FRN 8B	1,502.25	75/225	1200	2	2	1	265/130	305	420/200	650	150/150	1250/750	30/20
B5		3/4.5	115/260	1470	2	2	1	350/250	600	370/370	740	130/130	1000/530	25/20
B6	FRN 9A	1,250.3	150/260	1260	2	2	1	300/200	500	400/200	600	140/140	1300/600	50/30
B7	FRN 10	2/5	225/264	1870	2	2	1	230/200	430	500/250	750	225/225	1480/830	40/20
B8	GYRE 7, 8	5/11	200/300	1850	3	3	1	350/50	750	300/150	950	200/100	1000/500	100/30
B9	FRN 12	3.5/5.1	412/480	1350	3	3	1	220/100	520	300/150	750	100/100	1000/500	80/20
B10	GYRE 11, 12	8/15	600/900	1800	5	5	1	350/0	550	400/0	600	700/0	1500/400	60/20
B11		3/3.7	560											
B12		2,744.5	375/488	1150	2	2	1	150/150	300	400/200	600	250/250	1800	50/20
B13	GYRE 15	6/11	300/600	1825	4	4	1	300/100	750	315/135	775	300/20	800/500	50/30
B14	FRN 16	1,52/4.7	300	1100-1650	2	2	1	480/230	620	400/300	700	400/270	750/300	40/20
B15		2,7/2.7												
E1	FRN 4, 5	5/5	150/200	1325	3	3	1	450/150	600	450/175	425	300/300	1900/500	45/20
E2	FRN 6	4.5/4.5	260	1320	3	3	1	170/125	420	170/80	550	350/350	1750/1000	50/30
E3	GYRE 2, 3	7/7	350	1350	2	2	1	400/150	550	400/150	450	350/300	1200/600	60/30
E4	FRN 9B	2/5	340/600											
E5		6/6	400/600											

Table 1: Bryant and East canyons mini-basin morphology, depositional facies, and channel thalweg characteristics. Basin B12 comment: Channel thalwegs in channelized facies cannot be determined because of hyperbolic reflections. Seismic profiles (e.g., FRN4, etc) listed in table can be observed in the center panel.

Table 2

CANYON LOCATION	PROFILE EXAMPLE	CANYON FLOOR WIDTH (m)	CANYON WALL RELIEF (m)	CANYON CENTER DEPOSIT THICKNESS (m)	CANYON FACIES UNITS AND NUMBER OF UNITS	MTD	CHANNELIZED	FACIES UNIT THICKNESS CANYON CENTER (m)				CHANNEL SIZE			
								PONDING THICKNESS (m)	MTD	CHANNELIZED	MTD	CHANNELIZED	WIDTH (m)	RELIEF (m)	Comment
BRYANT CANYON PATHWAY															
UPPER SLOPE															
445 m	FRN 18	7.1	170	1130	NONE	1	1	NONE		250	170	800	1400	600	40
355 m	FRN 2	5	113/300	1000	NONE	1	1	NONE		150	150	150	1400	600	40
275 m	FRN 3	8.72	150/330	750	1	1	1	250	100	250	170	250	200	750	35
87.5 m	FRN 10	1.8	200/300	1350	2	2	1	300	100	300	120	400	400	1200	50
86.9 m	FRN 10/12/16	1.3	103/370	850	2	2	1	180	170	170	170	170	170	170	25
BRYANT CANYON MOUTH															
277.5 m	FRN 18	1	375/415	1050	1+	1+	1	300		300	380	300	350	450	1
EAST CANYON PATHWAY															
UPPER SLOPE															
677 m	FRN 1A	9	75	800	NONE	1	1	NONE		200	180	700	700	1700	40
750 m	FRN 2	8	75/200	800	NONE	1	1	NONE		150	150	450	450	2000	80
800 m	FRN 3	2.4	151/300	750	1	1	1	200	200	200	200	150	1000	400	30
E.3, 1275 m	FRN 9B	1.4	300	1050	2	2	1	200	100	200	300	300	300	1700	60
E.4, 1000 m	FRN 9B	1.8	300	1250	1	2	1	400	150	550	250	150	440	230	30

Table 2: Bryant and East canyons floor morphology, depositional facies, and channel characteristics. Seismic profiles (e.g., FRN4, etc) listed in table can be observed in the center panel.

Turbidite System	Channels Studied	Relief (m) max.	Width (m) max.	Seismic Facies
BRYANT CANYON	75	50-100	1000-2400	X X X
EAST CANYON	20	50-90	1000-2000	X X X
MISS. CANYON	1	75	1000+	X X X
TAHOE CHANNEL	1	80-120	1100	X X X
AUGER	20		750-2000	X X X
SUM 16 BASINS	-50	15-140	100-2500	X X X

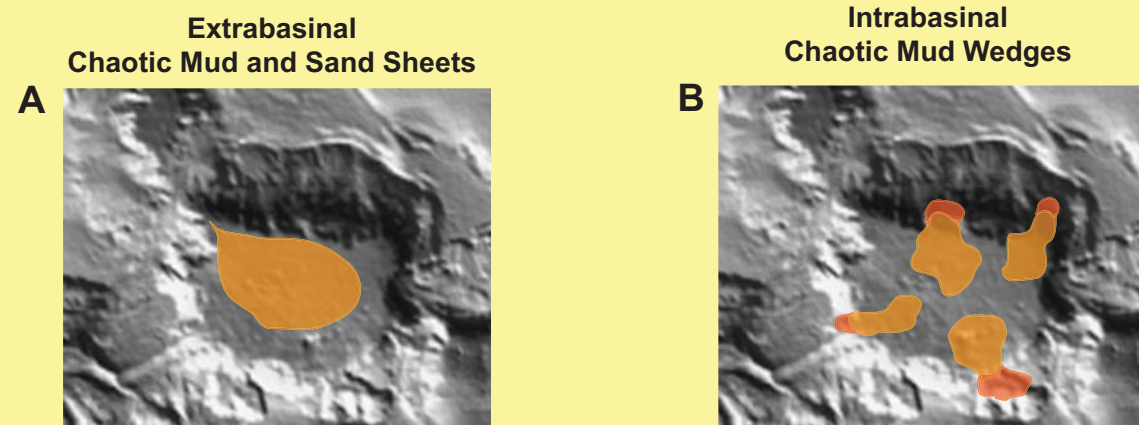
Table 3: Comparison of GOM mini-basin subsurface channel thalweg characteristics. Bryant and East canyons channel dimensions are from Tables 1 and 2 above; Mississippi Canyon, Tahoe, and Suger channel dimensions are from Kendrick (2000); Summary of 16 basins are from Shanley et al. (2000).

References

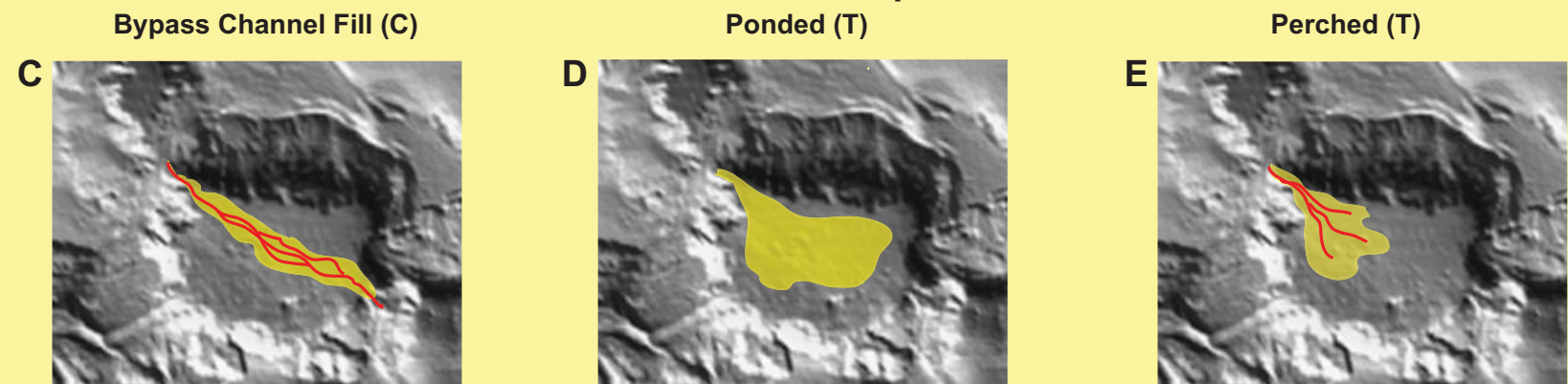
- Badalini, G., B. Kneller and C. D. Winker, 2000, Architecture and processes in the late Pleistocene Brazos-Trinity turbidite system, Gulf of Mexico, in P. Weimer, R.M. Slatt, J. Coleman, N.C. Rosen, C.H. Nelson, A.H. Bouma, M.J. Stytzen and D.T. Lawrence, eds., Deep-water Reservoirs of the World, 20th Annual Research Conference, Gulf Coast Section Society of Economic Paleontologists and Mineralogists, 16-34.
- Beaubouef, R.T. and S.J. Friedmann, 2000, High resolution seismic/sequence stratigraphic framework for the evolution of Pleistocene intra slope basins, Western Gulf of Mexico: Depositional models and reservoir analogs, in P. Weimer, R.M. Slatt, J. Coleman, N.C. Rosen, C.H. Nelson, A.H. Bouma, M.J. Stytzen and D.T. Lawrence, eds., Deep-water Reservoirs of the World, 20th Annual Research Conference, Gulf Coast Section Society of Economic Paleontologists and Mineralogists, 40-60.
- Damuth, J.E., and H.C. Olson, 2015, Latest Quaternary sedimentation in the northern Gulf of Mexico intraslope Basin Province: I. Sediment facies and depositional processes: Geosphere, 11, 1689-1718.
- Expedition 308 Scientists, 2005, Overpressure and fluid flow processes in the deepwater Gulf of Mexico: slope stability, seeps, and shallow-water flow: Integrated Ocean Drilling Program Preliminary Report, 308.
- Liu, J.Y., and W.R. Bryant, 2000, Seafloor relief of northern Gulf of Mexico deep water: Texas Sea Grant College Program.
- Olson, H.C., J.E. Damuth and C.H. Nelson, 2016, Latest Quaternary sedimentation in the Northern Gulf of Mexico intraslope Basin Province: II. Stratigraphic analysis and relationship to glacioeustatic climate change: Interpretation, 4, 8C81-8C95.
- Prather, B.E., J.R. Booth, G.S. Steffens and P.A. Craig, 1998, Classification, lithologic calibration, and stratigraphic succession of seismic facies of intraslope basins, deep-water Gulf of Mexico: AAPG Bulletin, 82, 701-728.
- Sandwell, D.T., and W.H. Smith, 1997, Marine gravity anomaly from Geosat and ERS 1 satellite altimetry: Journal of Geophysical Research: Solid Earth, 102, no. B5, 10039-10054.
- Suter, J.R., 2003, Later Quaternary Shelf Margin Deltas, Northern Gulf of Mexico, in H.H. Roberts, N.C. Rosen, R.H. Fillon, and J.B. Anderson, eds., Shelf margin deltas and linked down slope petroleum systems: Global significance and future exploration potential: Gulf Coast Section SEPM Foundation 23rd Annual Research Conference, 27-43.
- Tripanas, E.K., W.R. Bryant and B.A. Phaneuf, 2004a, Slope instability processes caused by salt movements in a complex deep-water environment, Bryant Canyon Area-Northwest Gulf of Mexico: AAPG Bulletin, 88, 801-823.
- Tripanas, E.K., W.R. Bryant and B.A. Phaneuf, 2004b, Depositional processes of uniform mud deposits (unifites), Hedberg Basin, Northwest Gulf of Mexico, New Perspectives: AAPG Bulletin, 88, 825-840.
- Twichell, D.C., C.H. Nelson, J.E. Damuth and L.F. Pratson, 2000, Distribution and late-stage development of a turbidite pathway on the Louisiana continental slope, in P. Weimer, R.M. Slatt, J. Coleman, N.C. Rosen, C.H. Nelson, A.H. Bouma, M.J. Stytzen, and D.T. Lawrence, eds., Deep-water reservoirs of the world: Gulf Coast Section SEPM Foundation 20th Annual Research Conference, 1032-1044.

Types of Bryant Canyon Mini-Basin Deposits

Mass-Transport Deposits (MTD)



Turbidite Sand Deposits



Schematic diagram showing the types of deposits that form the depositional facies units (MTD, T, and C) in the Bryant Canyon mini-basin deposits based interpretation of seismic facies (center panel). MTDs are orange shades, turbidites are yellow shades, and channels are bright red. The bathymetric map is Beaumont Basin and is from the bathymetric maps in the center panel. These deposits and depositional facies are characteristic of other Miocene-to-present-age GOM mini-basins.

Conclusions

- Two major types of mini-basin deposits are recognized in the Bryant Canyon Turbidite System: (1) mass-transport deposits (MTD facies units) and (2) sandy turbidite deposits (T facies units) (No. 13 above). Extrabasinal MTDs are derived from upstream allocthonous shelf-margin delta or canyon-wall failures generally consist of massive chaotic mud-clast debris flows. However, some are sandy debris flows and may provide subsurface reservoirs. Extrabasinal MTD facies may be ponded at inlets or outlets. In contrast, muddy intrabasinal MTD wedges are derived from local canyon wall failures, are dominantly clay-rich, may be intruded into other basin units and commonly form capping units to mini-basin deposits. Clay-rich intrabasinal and extrabasinal MTD facies can seal underlying T facies units, but sandy extrabasinal MTD facies units may not seal T facies.
- In the Bryant Canyon area, the robust salt tectonics result in greater mini-basin relief and more MTD deposits than in subsurface mini-basins to the east or west, where more amalgamated T facies units are encountered. Extrabasinal MTDs derived from upstream allocthonous shelf-margin delta or canyon-wall failures generally consist of massive chaotic mud-clast debris flows. However, some are sandy debris flows and may provide subsurface reservoirs. Extrabasinal MTD facies may be ponded at inlets or outlets. In contrast, muddy intrabasinal MTD wedges are derived from local canyon wall failures, are dominantly clay-rich, may be intruded into other basin units and commonly form capping units to mini-basin deposits. Clay-rich intrabasinal and extrabasinal MTD facies can seal underlying T facies units, but sandy extrabasinal MTD facies units may not seal T facies.
- Bryant Canyon sand-rich turbidite deposits located at the canyon inlets to mini-basins may be incised, bypass channel fill, perched fans or ponded facies. Deposits at outlets may be ponded or incised. A wide variation (~15-100%) in net-to-gross sand content is expected in turbidite deposits (T facies units). Thus along Bryant Canyon, multiple mini-basins can fill and spill rapidly during one phase of glacio-eustatic sea-level lowering.
- Similar mini-basin turbidite systems have been deposited by ancestral Mississippi shelf-margin deltas that fed the Mississippi Canyon area during the Miocene and then migrated west to Alaminos Canyon during the Pliocene through the Pleistocene Penultimate Glacial (MIS 6) (See No. 4 in left panel). The Bryant mini-basins thus provide good modern analogues for the subsurface Miocene-to-Pleistocene mini-basins in the intraslope basin province. In contrast, the Mississippi Fan turbidite system deposited during the late Last Glacial (MIS 2) is not a good analogue for Miocene-to-Penultimate Glacial (MIS 6) turbidite systems because the Mississippi drainage switched to the east of the intraslope basin province, doubled in size, became finer grained, and fed sediments to the large modern Mississippi Canyon where no mini-basins were present.
- The Bryant mini-basins exhibit the same seismic facies units (MTD, C, T), scale of basin sizes, facies thicknesses and channel morphology as the subsurface Miocene-to-Pleistocene mini-basins (see Tables 1-3, this panel). The inlet (incised, bypass channel fill, perched or ponded) depositional facies interpreted as ponded turbidite facies also are similar in Bryant, Brazos-Trinity and subsurface Miocene-to-Pleistocene mini-basins. In both the modern and subsurface mini-basins, if basin walls had high relief, muddy suspension flows could not overflow the walls (via flow stripping), and thus, could not exit the basins. Thus, more mud-rich ponded turbidites would have been deposited. If mini-basin walls had relatively lower relief, greater flow stripping may have occurred and younger sand-rich ponded turbidites were deposited.

NOTE: A detailed discussion of deposition in Beaumont Basin is given in our paper that is published in the May 2018 volume of Interpretation: Nelson, C.H., Damuth, J.E., and Olson, H.C., 2018, Late Pleistocene Bryant Canyon turbidite system: Implications for Gulf of Mexico minibasin petroleum systems; Interpretation, V. 6, No. 2, (May 2018), p. 1-26.